Low Reynolds number k-ε modeling by using the direct numerical simulation (DNS) data

Ahmed Abdul-Hussein Ouda

Thi-Qar university - college of science - computer dept.

Abstract:

The constant C_μ and the near-wall damping function f_μ in the eddy-viscosity relation of the k-ε model are evaluated from direct numerical simulation (DNS) data for developed channel and boundary-layer flow, each at two Reynolds numbers. Various existing f_μ model functions are compared with the DNS data, and a new function is fitted to the high-Reynolds-number channel flow data. The ε-budget is computed for the fully developed channel flow. The relative magnitude of the terms in the ε-equation is analyzed with the aid of scaling arguments, and the parameter governing this magnitude is established. Models for the sum of all source and sink terms in the ε- equation are tested against the DNS data, and an improved model is proposed.

1. Introduction

The k-ε model has become one of the most popular turbulence models used regularly in many calculations of flows of practical interest. In the past, k-ε model calculations were mostly carried out in conjunction with wall functions bridging the viscosity affected near-wall region. Recently, however, low-Reynolds-number *(low-Re)* versions of the k-ε model are being used in which the near-wall region is resolved. These versions contain damping functions and extra terms in order to account for the observed near-wall effects,and, in most cases, these terms and functions have been made to depend on the viscosity. A wide variety of model versions has been proposed in the literature. The pre-1984 models were reviewed in Patel, Rodi & Scheuerer (1985). Since then, a number of newer proposals have emerged (see e.g. Shih & Mansour 1990).

The extra terms and functions in *low-Re* k-ε models have not been derived on the basis of data but on various modeling arguments, and they have only

been subjected to indirect testing by calculating various flows with the models. The same is true for the entire ε-equation, even the high Reynolds number *(high-Re)* version, which must be considered empirical. Direct numerical simulation (DNS) data are now available with which the individual model assumptions can be tested directly. The data can also be used as a basis for the development of improved models. The DNS data available are still for flows at fairly low Reynolds numbers, but they are suitable for examining the near-wall behavior of models and for aiding the development of realistic models in this region.

In the president work, two main issues were investigated with the aid of DNS data. The first one is the behavior of the coefficient in the eddy-viscosity expression in *k-ε* models, particularly near walls. The second issue is the model form of the *ε*-equation. For high Reynolds numbers, where the energy-containing and dissipative motions are very different in scale, the exact ε-equation provides little if any guidance.

(a)	k	ε	$\tilde{\varepsilon}$	v_t	$\overline{u'v'}/k$	p/ε	R	R_g
	$O(y^2)$	$O(1)$	$O(y^2)$	$O(y^3)$	$O(y)$	$O(y^2)$	$O(1)$	$O(y)$
(b)	P_ε^1	P_ε^2	P_ε^3	P_ε^4	T_ε	Π_ε	D_ε	Y
	$O(y)$	$O(y^2)$	$O(y^2)$	$O(y)$	$O(y)$	$O(1)$	$O(1)$	$O(1)$

TABLE 1. *(a)* Summary of near-wall behavior of various quantities. *(b)* Summary of near-wall behavior of the terms in the ε-budget. RODI (2000).

But in low-Reynolds-number regions near walls the situation is different because the scales of energy-containing motions and the scales of dissipative motions are the same (Launder 1986). In this case, the exact ε-equation is useful for identifying and describing the

various near-wall influences on ε. The terms in the exact ε-equation cannot be measured and therefore information on these terms can only be obtained from DNS data. The data used in this work were for developed channel flow (Kim, Moin & Moser 1987; J. Kim 1990, unpublished data) and for boundary layers in zero pressure gradient (Spalart 1988), each at two Reynolds numbers. The dissipation rate budget could only be computed for the developed channel flow case. For
the lower Reynolds number $(Re_\tau = 180$ based on friction velocity and channel half-width), Mansour, Kim & Moin (1988) have already provided the ε-budget and tested some model approximations. Here, the ε-budget is provided for Kim's (1990, unpublished data) new channel flow calculations at $Re_\tau = 395$. Some of the more successful *low-Re k-ε* model versions are tested against these data and new model proposals are made for the source/sink terms in the ε-equation.

2. Form of low Reynolds number *k-ε* models:

The *k*-ε model employs the eddy-viscosity concept, and for the various *low-Re k*-ε models proposed so far the relations for determining the eddy viscosity *vt* can be written for two-dimensional shear layers in the following form:

$$v_t = C_\mu f_\mu k^2/\tilde{\varepsilon}, \tag{1}$$

$$\frac{D}{Dt}k = \left[\left(v+\frac{v_t}{\sigma_k}\right)k_{,j}\right]_{,j} + v_t(U_{,j})^2 - \varepsilon, \tag{2}$$

$$\frac{D}{Dt}\varepsilon = \left[\left(v+\frac{v_t}{\sigma_\varepsilon}\right)\tilde{\varepsilon}_{,j}\right]_{,j} + C_{\varepsilon 1}f_1\frac{\tilde{\varepsilon}}{k}v_t(U_{,j})^2 - C_{\varepsilon 2}f_2\frac{\tilde{\varepsilon}^2}{k} + E, \tag{3}$$

$$\tilde{\varepsilon} = \varepsilon - D. \tag{4}$$

The various models differ through the use of different functions f_μ, f_1, f_2 and different terms **D** and **E**. In the eddy-viscosity relation (1), C_μ is a constant coefficient while f_μ. is a damping function reducing the eddy viscosity near the wall. Some models use as turbulence timescale k/ε and solve an equation for ε itself (effectively putting D to zero), while other models use as timescale k/ε and solve an equation for

Model	Code	D	$\tilde{\varepsilon}_w/BC$	C_μ	$C_{\varepsilon 1}$	$C_{\varepsilon 2}$	σ_k	σ_ε	E
(a) Launder-Sharma	LS	$2\nu(k_{,y})^2$	0	0.09	1.44	1.92	1.0	1.3	$2\nu\nu_t(U_{,yy})^2$
Chien	CH	$2\nu k/y^2$	0	0.09	1.35	1.8	1.0	1.3	$-2\nu\tilde{\varepsilon}/y^2\exp(-0.5y^+)$
Lam-Bremhorst	LB	0	$\nu k_{,yy}$ or $\varepsilon_{,y}=0$	0.09	1.44	1.92	1.0	1.3	0
Shih-Mansour	SM*	$2\nu(k_{,y})^2$	$\nu k_{,yy}$	0.09	1.45	2.0	1.3	1.3	$\nu\nu_t(U_{,yy})^2$
Nagano- Tagawa	NT	0	$\nu k_{,yy}$	0.09	1.45	1.9	1.4	1.3	0

Model	Code	f_μ	f_1	f_2
(b) Launder-Sharma	LS	$\exp(-3.4/(1+Re_t/50)^2)$	1.0	$1-0.3\exp(-Re_t^2)$
Chien	CH	$1-\exp(-0.0115y^+)$	1.0	$1-0.22\exp(-(Re_t/6)^2)$
Lam-Bremhorst	LB	$[1-\exp(-0.0165y^*)]^2(1+20.5/Re_t)$	$1+(0.05/f_\mu)^3$	$1-\exp(-Re_t^2)$
Shih-Mansour	SM*	$[1-\exp(-a_1y^*-a_3y^{*3}-a_5y^{*5})]^{1/2}$	1.0	$(1-0.22\exp(-(Re_t/6)^2))\tilde{\varepsilon}/\varepsilon$
Nagano- Tagawa	NT	$[1-\exp(-y^*/26)]^2(1+4.1/Re_t^{3/4})$	1.0	$(1-0.3\exp(-(Re_t/6.5)^2))(1-\exp(-y^*/6))^2$

TABLE 2. *(a)* Summary of constants, terms and boundary conditions used in existing *low-Re k-e* models. *(b)* Summary of damping functions used in existing *low-Re k-ε* models $(Re_t = k^2/\nu\varepsilon$, $y^+ = U_\tau y/\nu$, $y^* = k^{1/2}y/\nu)$.

*SM solve forε rather than *e*, but they useε to define the eddy viscosity. RODI (2000).

the isotropic part of the dissipation $\tilde{\varepsilon}$ which, in contrast to ε, goes to zero at the wall. For convenience, the near-wall behavior of various parameters in the model is given in table 1. The function f_2 in the $\tilde{\varepsilon}$ -equation is usually effective only very close to the wall and is introduced to simulate the change in the decay rate of homogeneous turbulence as the Reynolds number $Re_t(= k^2/\nu e)$ becomes small. In the case where an equation for ε itself is solved, f_2 must, in addition, prevent the sink term

involving ε^2/k becoming infinite at the wall (i.e. $f_2 \sim y^2$ as $y\rightarrow0$). The extra term ε or alternatively the function $f1$ were introduced to increase the e-production near the wall. A general discussion on the functions and extra terms in the various models proposed until 1984 can be found in Patel *et al.* (1985). Here, attention is focused on the damping function f_μ and on the ε-equation (3), and with the aid of DNS data the performance of five *low-Re k-ε* models is examined. These are the models due to Launder & Sharma (1974, hereafter referred to as LS), Lam & Bremhorst (1981, hereafter referred to as LB) and Chien (1982, hereafter referred to as CH) rated best in the review article of Patel *et al.* (1985), and the more recently proposed models of Shih & Mansour (1990, hereafter referred to as SM) and Nagano & Tagawa (1990, hereafter referred to as NT). The constants and functions used in these five models are compiled in table 2. It should be mentioned that the SM model involves an additional pressure-diffusion term in the *k*-equation (2).

All of the models considered are of the form such that when f_μ, f_l, f_2 are set to 1, and terms D andε are set to zero, the standard high-Re version of the *k-ε* model is recovered.

3. C_μ constant and f_μ function:

With $C_\mu = 0.09$ chosen as used in standard *k-ε* models, the function f_μ in the eddy- viscosity relation (1) was determined from DNS data for both developed channel flow and boundary-layer flow at the two Reynolds numbers. The resulting f_μ distributions are plotted versus $y^+ = U_\tau y/\nu$ in figure 1. Away from the wall, the!;.distribution gives an indication of the value of C_μ, which should be constant ($f_\mu = 1.0$ when $C_\mu =$

0.09). Indeed, figure 1 (a) shows, for the higher-Reynolds-number channel flow, that C_μ is roughly 0.09 over more than three quarters of the channel depth. It should be noted that this is in contrast to Rodi's (1975) evaluation of Laufer's (1954) experimental pipe-flow data which show C_μ to increase towards the pipe axis where the ratio of production to dissipation of turbulence energy, P/ε, goes to zero. For the channel with $Re_\tau = 180$, a higher C_μ value results in the central part of the channel. In contrast, the C_μ value in the boundary layer, not too close to the wall, is only approximately 0.075. The behavior of C_μ (or rather $C_\mu f_\mu$) can be explained via the distributions of $\overline{u'v'}/k$ and P/ε since (1) and (2) can be combined to yield

$$f_\mu C_\mu = \left(\overline{u'v'}/k\right)^2 (P/\varepsilon). \qquad (5)$$

$C_\mu = 0.09$ (with $f_\mu = 1$) corresponds to $P/\varepsilon = 1$ (local equilibrium) and the often measured value of the structure parameter $-\overline{u'v'}/k = 0.3$. Figures 2 and 3 show respectively, again for channel and boundary-layer flows, the distributions of the parameters $-\overline{u'v'}/k$ and P/ε determining $C_\mu f_\mu$ according to relation (5). In the low-Re channel, the ratio P/ε has a value of only about 0.85 in the region where $-\overline{u'v'}/k \approx 0.3$, which explains the higher $C_\mu f_\mu$ value. In the high-Re channel, P/ε drops faster than $-\overline{u'v'}/k$ towards the channel centre so that $(\overline{u'v'}/k)^2 /(P/\varepsilon) \approx$ constant, which explain the constant value of $C_\mu f_\mu$ in the central portion of the channel. In the boundary layer. $-\overline{u'v'}/k$ approaches 0.3 only where the ratio P/ε is significantly larger than 1, which leads to the relatively low value of $C_\mu f_\mu \approx 0.075$ over

larger parts of the boundary layer. More towards the edge of the boundary layer, where P/ε tends to zero, $C_\mu f_\mu$ Increases.

The foregoing has shown that the use of a constant value of $C_\mu = 0.09$ can generally be only a rough approximation. When this value is chosen and when f_μ is introduced
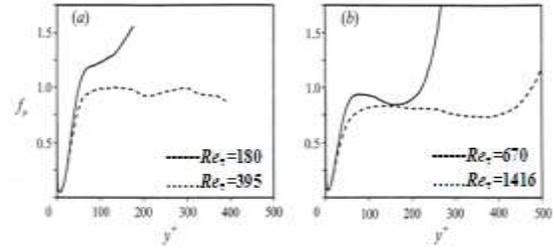

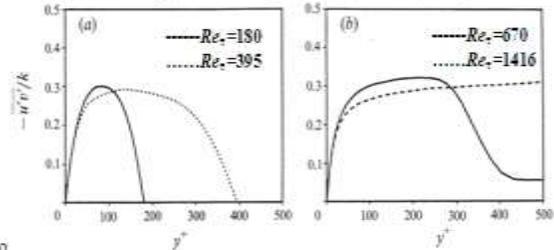FIGURE 1. f_μ-distribution ($f_\mu = \nu_t \varepsilon / C_\mu k^2$ with $C_\mu = 0.09$).

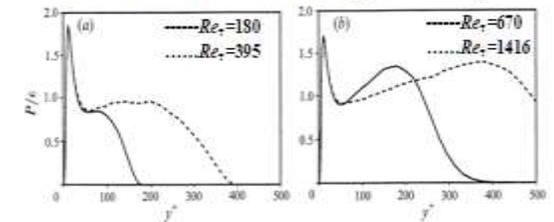FIGURE 2. Distribution of the structure parameter $-\overline{u'v'}/k$.

FIGURE 3. Distribution of the ratio of production to dissipation of turbulent kinetic energy, P/ε.

to represent the damping of the eddy viscosity near the wall, then f_μ must take a value of 1 away from the wall, which of course cannot agree with all the DNS data. For the near-wall region ($y^+ < 100$) in channel flow, figure 4 compares the f_μ functions due to LS, LB, CH, SM and NT with the DNS data for both Reynolds numbers, and figure 5 provides a similar comparison for the higher-Reynolds-number boundary-layer flow.
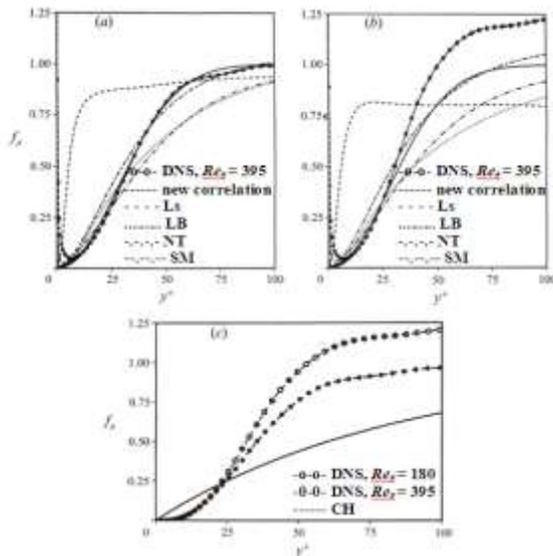
FIGURE 4. Comparison of various f_μ-model functions with DNS data for channel flow.

Very near the wall, two sets of DNS data have to be distinguished: one using ε itself in the eddy-viscosity relation (1) which causes f_μ to behave as $1/y$ since ε is finite at the wall; the other is based on the use of the modified dissipation rate $\tilde{\varepsilon}$ which varies as . very near the wall so that f_μ goes to zero at the wall as y. The LS, CH and SM mode use $\tilde{\varepsilon} \neq \varepsilon$ in (1) so that their f_μ functions should and do go to zero at the wall. However, the CH function can be seen to rise and approach the value of unity far too slowly, while the LS function initially rises far too quickly but then also has a rather slow approach to the value of 1. That the f_μ function due to LS never rises beyond 0.8 for the *low-Re* channel case is due to the fact that the argument of the f_μ function, Re_t , rises to a maximum at $y^+ \approx 20$ and then falls again. The SM function also approaches the

value of 1 too slowly. The models of LB and NT use ε and hence f_μ should increase very close to the wall; the f_μ function due to NT does so and, overall, fits the high-Re channel DNS data quite well, being only slightly higher in the region.
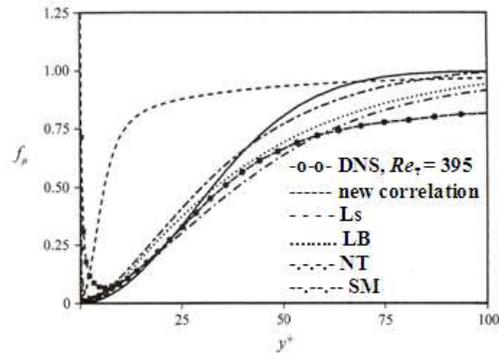

FIGURE 5. Comparison of variousJ;.-model functions with DNS data for boundary layer (Re_θ =1416).

$10 < y^+ < 40$. On the other hand, the LB f_μ function goes to zero at the wall, which causes v_t to behave as y^4 instead of y^3. The following increase in f_μ is simulated fairly well by the LB function, but then it approaches unity somewhat too slowly. The fairly good agreement for the boundary layer (figure 5) is somewhat misleading because the far-wall value of the data is lower than I. There seems to be some influence of the Reynolds number on the f_μ distribution in f_μ *vs.* y^+ plot, but in view of the differences between various wall-bounded flows, the inclusion of such effects in a single model is not warranted. Hence, a y^+-dependent f_μ function based on the data for the high-Re channel flow appears as a reasonable compromise, and by curve-fitting, the following f_μ function has been determined:

$$f_\mu = 1 - exp(-0.0002y^+ - 0.00065y^{+2}). \qquad (6)$$

This relation, which is also included in figures 4 and 5, is only suitable for attached flows, while in separated flows the argument y^+ should be replaced by $Re_y = k^{1/2}y/\nu$. It should be noted that the f_μ-function (6) has the correct near-wall behavior ($f_\mu \sim y$) in connection with the use of $\tilde\varepsilon$ in (1).

This relation, which is also included in figures 4 and 5, is only suitable for attached flows, while in separated flows the argument y^+ should be replaced by $Re_y = k^{1/2}y/\nu$. It should be noted that the f_μ-function (6) has the correct near-wall behavior ($f_\mu \sim y$) in connection with the use of $\tilde\varepsilon$ in (1).

Durbin (1990) suggested the use of the normal fluctuations $(\overline{v'^2})^{1/2}$ as velocity scale in the eddy-viscosity relation (1) instead of $k^{1/2}$ and argued that a damping function would not be needed in this case. His eddy-viscosity relation reads

$$v_t = C\mu \overline{v'^2} T, \qquad (7)$$

with the time-scale T determined from

$$T = \max\left(\frac{k}{\varepsilon}, 6\left(\frac{\nu}{\varepsilon}\right)^{1/2}\right). \qquad (8)$$

It has already been shown by Launder (1986) that the near-wall damping expressed through the function f_μ in (1) is due not so much to viscous effects but to the damping of the normal fluctuations v' by the pressure-reflection mechanism and that f_μ therefore correlates very well with $\overline{v'^2}/k$. Hence it is interesting to test Durbin's model proposal (7) with the aid of DNS data. Figure 6 shows C_μ in relation (7) determined from the channel-flow data at two Reynolds numbers. It can be seen that C_μ is indeed fairly constant down to $y+ \approx 10$. The C_μ value depends somewhat on the Reynolds number as noted

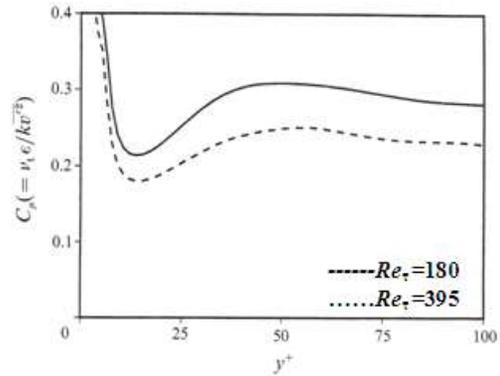already in the context of Cl'' appearing in (1).

FIGURE 6. Distribution of C_μ in Durbin's (1990) model.

Very close to the wall, where the timescale T according to (8) adopts a finite value, C_μ behaves as $1/y$. The use of a constant C_μ leads to $v_t \propto y^4$ and the correct v_t-distribution near the wall ($v_t \propto y^3$) can only be obtained by introduction of a damping function in this region.

4. The ε-budget

The exact equation for $\varepsilon(= \nu\overline{u'_{i,j}u'_{i,j}})$ derived from the Navier-Stokes equations can be written in tensor form as

$$\frac{D}{Dt} = P_\varepsilon^1 + P_\varepsilon^2 + P_\varepsilon^3 + P_\varepsilon^4 + T_\varepsilon + \Pi_\varepsilon + D_\varepsilon - Y \qquad (9)$$

where the individual terms on the right-hand side are defined and identified as

$P_\varepsilon^1 = -\nu 2\overline{u'_{i,j}u'_{k,j}}S_{ik}$ Mixed production,

$P_\varepsilon^2 = -\nu 2\overline{u'_{i,k}u'_{i,m}}S_{km}$ Production by mean velocity gradient,

$P_\varepsilon^3 = -\nu 2\overline{u'_j u'_{i,m}}U_{i,km}$ Gradient production,

$P_\varepsilon^4 = -\nu 2\overline{u'_{i,k}u'_{i,m}u'_{k,m}}$ Turbulent production,

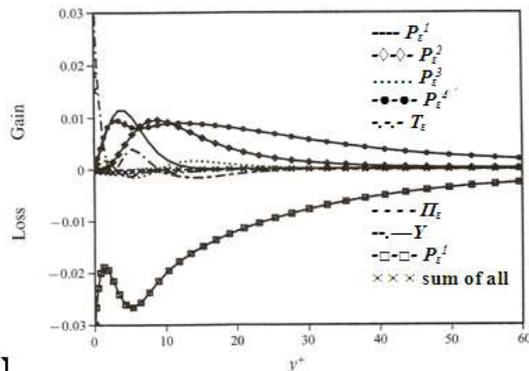$T_\varepsilon = -\nu\left(\overline{u'_k u'_{i,m}u'_{k,m}}\right)_{,k}$ Turbulent transport,

$$\Pi_\varepsilon = -v \frac{2}{\rho} \left(\overline{p'_{,m} u'_{k,m}} \right)_{,k}$$ **Pressure transport**

$$D_\varepsilon = v \varepsilon_{,kk}$$ **Viscous diffusion,**

$$Y = v^2 \, 2 \overline{u'_{i,km} u'_{i,km}}$$ **Dissipation.**

and $S_{ij} = \frac{1}{2}(U_{i,j} + U_{j,i})$ **is the mean strain rate. For developed channel flow, the left hand side is zero so that the terms on the right-hand side should balance each other. The near-wall behavior of the individual terms is given in table 1 *(b)*. Mansour *et al.* (1988) have calculated the ε-budget from the DNS data for the *low-Re* channel flow. The *ε*-budget evaluated from the data for the channel with $Re_\tau = 395$ is given in figure 7. All terms have been made dimensionless with U_τ^6/v^2. The imbalance in the budget (crosses) is also given; this is a measure of the errors in the budget terms due to discretization and limited sample size.**

FIGURE 7. ε-budget for channel flow at $Re_\tau = 395$.

As can be seen, the imbalance is fairly small relative to the terms in the budget, except very close to the wall. This imbalance is small relative to the imbalance between the production and dissipation for $y^+ > 8$, so that the ε-budget determined from the DNS data can be considered accurate for $y^+ > 8$. Taking the Chebychev transform of all

the terms in the ε-budget reveals that the major source of error is from computing the dissipation rate *(Y)* of ε which is under-resolved near the wall. However, it should be emphasized here that ε itself and also ε determined from the DNS data are accurate down to the wall.

As was to be expected from the order-of-magnitude analysis of Tennekes & Lumley (1972), the turbulent production rate P_ε^4 due to vortex stretching and the viscous destruction *Y* dominate the balance equation in the high-Reynolds-number region away from the wall. However, near the wall, the production terms P_ε^1 and P_ε^2 become equally important, and at the wall itself viscous destruction is balanced by viscous diffusion and pressure transport. The smaller terms, P_ε^3, T_ε and Π_ε are shown in figure 8 on an expanded scale. The imbalance can be seen to be small even compared with these small terms for $y^+ > 8$, and the pressure diffusion Π_ε can be seen to be negligible everywhere. On the other hand, the relatively small production term P_ε^3 is of the same order of magnitude as the turbulent diffusion T_ε

The terms P_ε^4 and *Y* increase with increasing Reynolds number, but their difference remains independent of Reynolds number (once this is sufficiently high); the latter is true also for the rate of change and transport terms, of which in the channel flow situation only the diffusion term is non-zero. According to Tennekes&Lumley (1972), the terms P_ε^1 and P_ε^2 relative to the difference $(P_\varepsilon^4 - Y)$ are of order $1/Re^{1/2}$. Figure 9 shows the sum $P_\varepsilon^1 + P_\varepsilon^2$ and the difference $P_\varepsilon^4 - Y$ for channel flow at both Reynolds numbers investigated. With the non-dimensionalization chosen, there is no noticeable Reynolds-number

influence on either group of terms away from the wall. Near the wall, both groups increase somewhat with the Reynolds number. Also, it is clear that the destruction term Y adjusts to the increase of ε-production due to P_ε^1 and P_ε^2 near the wall and in fact tends to over-react somewhat. The sum of all source and sink terms (i.e. $P_\varepsilon^1 + P_\varepsilon^2 + P_\varepsilon^3 + P_\varepsilon^4 - Y$) is also included in figure 9.
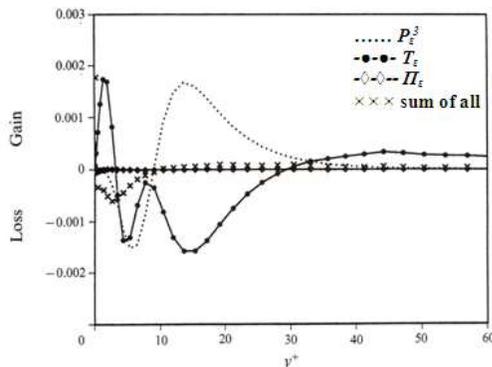

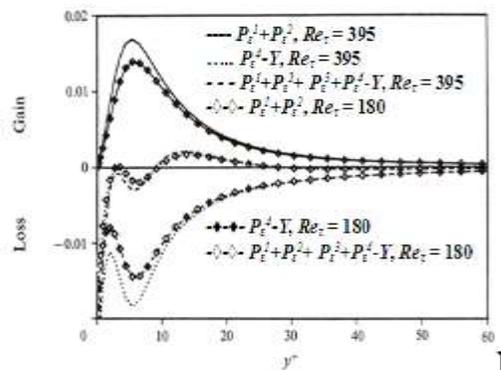**FIGURE 8. Small terms in the ε-budget for channel flow at $Re_\tau = 395$.**

FIGURE 9. Distribution of $P_\varepsilon^1 + P_\varepsilon^2$, J>;-land sum of all source and sink terms in channel flow.

This sum, which is little influenced by the Reynolds number, is very small compared with the actual terms in the ε-equation. It is this sum which, in general, balances the rate of change, convective and diffusive transport terms in the ε-equation and therefore governs the magnitude of ε. Hence it is only this

sum that really matters and has to be modeled. Because of the small magnitude of the net source compared with the original terms in the ε-equation, the usefulness of the exact ε-equation has sometimes been considered doubtful. However, even though this source is small it is still finite and balances the rate of change and transport of ε. At high Reynolds numbers, where an inertial sub range exists, the source/sink terms are given by the integral over the low-wave number part of the spectrum of the spectral transfer function multiplied by the wave number squared (see e.g. Rodi 1971). This shows that ε is governed by the larger-scale turbulent motions which are independent of Reynolds number.

5. Scaling arguments

Tennekes & Lumley (1972) made an order-of-magnitude analysis of the terms in the vorticity-fluctuation equation. The order of magnitude was expressed in terms of the velocity scale u, the macro-length scale l and the Taylor micro scale λ. They found that the relative magnitude of the individual terms and hence also the importance of the production terms P_ε^1 and P_ε^2 depends on the Reynolds number $Re_l = ul/v$. In a study of homogeneous shear flow, Bardina (1988) argued that the Reynolds number is not the only parameter determining the relative importance of the P_ε^1 and P_ε^2 production terms but that the mean shear number $S_n = Sk/\varepsilon$ plays also a role (S is the mean shear rate). His conclusions are of interest here, but his derivation seems not to be quite correct and also does not allow direct insight into the *Re-dependence* of the terms in the e-equation. Hence, scaling arguments are elaborated here once more.

Because of the close relation between the dissipation rate ε and the fluctuating vorticity $\overline{w_i' w_i'}$ (with $\varepsilon = \nu \overline{w_i' w_i'}$ in homogeneous flows) the scaling arguments of Tennekes & Lumley can be applied directly to the ε-equation. When the strain rate in the terms P_ε^1 and P_ε^2 is not expressed as u/l but is retained as a strain-rate parameter S (which is channel flow is equal to the shear rate a $\delta U/\delta y$) and with $\varepsilon \propto \nu u^2/\lambda^2 \propto u^3/l$ and the velocity scale $u = k^{1/2}$, the order of magnitude of the various terms follows as

$$P_\varepsilon^1, P_\varepsilon^2 = O\left(S \frac{k^{2/3}}{l} \frac{\lambda}{l} \right), \qquad (10)$$

$$P_\varepsilon^4, Y = O\left(\frac{k^2}{l^2} \frac{\lambda}{l} \right), \qquad (11)$$

$$P_\varepsilon^4 - Y, \frac{D}{Dt}\varepsilon, T_\varepsilon = O\left(\frac{k^2}{l^2} \right). \qquad (12)$$

Since $l/\lambda \propto Re_l^{1/2} \propto Re_t^{1/2}$, the terms P_ε^1 and P_ε^2 decrease as Ret increases, while the terms P_ε^4 and Y increase. The difference of the latter terms, P_ε^4-Y, and also the rate of change and transport terms are independent of Reynolds number, as mentioned already. The magnitude of the production terms P_ε^1 and P_ε^2 relative to the main terms in the model ε-equation (difference P_ε^4-Y and transport terms) can now be established as:

$$\frac{P_\varepsilon^1, P_\varepsilon^2}{P_\varepsilon^4 - Y} = O\left(\frac{Sk}{\varepsilon} \frac{1}{Re_t^{1/2}} \right). \qquad (13)$$

The relative order of magnitude of P_ε^1 and P_ε^2 is therefore determined by the parameter

$$R = \frac{Sk}{\varepsilon} \frac{1}{Re_t^{1/2}} = \frac{S}{(\varepsilon/\nu)^{1/2}}, \qquad (14)$$

which indeed involves the parameter $S_n = Sk/\varepsilon$. Relation (14) shows that the parameter R is the ratio of the timescale

of the dissipative motion to the timescale of the mean strain field. Bardina (1988) also arrived at this parameter, but his derivation concerns the ratio of order of magnitudes of terms P_ε^1 and P_ε^2 to P_ε^4 and Y, while here it represents the magnitude relative to the difference of the latter terms. The scaling arguments show that the production terms P_ε^1 and P_ε^2 are important when the parameter $R > 1$. Bardina (1988) examined two sets of homogeneous shear-flow data obtained by direct numerical simulations.
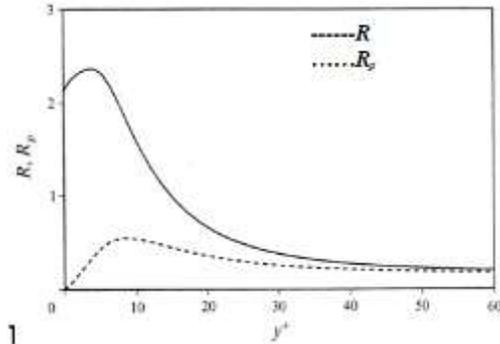

FIGURE 10. Distribution of parameters R and R_p in channel flow at $Re_\tau = 395$.

For low-shear cases with typically $R < 0.3$ the terms P_ε^1 and P_ε^2 were found small compared with P_ε^4 while for the case with high shear (and low Reynolds number) characterized by $R = 6$-15, the terms P_ε^1 and P_ε^2 were found to be larger than P_ε^4.

The distribution of the parameter R in the channel flow with $Re_\tau = 395$ is shown in figure 10. It can be seen that in the bulk of the channel flow the parameter is substantially below 1 (≈ 0.25). In the near-wall region, where the terms P_ε^1 and P_ε^2 become important, the parameter R increases strongly and reaches a maximum value of 2.4.

The above scaling arguments followed the assumption of Tennekes & Lumley (1972) that the anisotropic part of the

correlation $\overline{vu'_{i,j}u'_{i,m}}$ is proportional to $(uv/\lambda)(u/l) \propto \varepsilon/\ Re_t^{1/2}$. When u/l is retained as strain-rate parameter S (Mansour 1991), this correlation is proportional to $(uv/\lambda)(u/l) \propto (\varepsilon/\ Re_t^{1/2})\ (Sk/\varepsilon)$. The production terms P_ε^1 and P_ε^2 are then of order

$$P_\varepsilon^1, P_\varepsilon^2 = O\left(S^2 k \frac{\lambda}{l} \right) \qquad (15)$$

and the magnitude of these terms relative to the difference P_ε^4-Y is

$$\frac{P_\varepsilon^1, P_\varepsilon^2}{P_\varepsilon^4 - Y} = O\left(\left(\frac{Sk}{\varepsilon}\right)^2 \frac{1}{\text{Re}_t^{1/2}} \right) \qquad (16)$$

According to this scaling argument, the relative magnitude of P_ε^1 and P_ε^2 would therefore be determined by the parameter

$$R' = \left(\frac{Sk}{\varepsilon}\right)^2 \frac{1}{\text{Re}_t^{1/2}} \qquad (17)$$

With the shear stress $-\overline{u'v'} \propto (k^2/\varepsilon)S$, in the context of an eddy-viscosity model, and the production $P = -\overline{u'v'} \propto (k^2/\varepsilon)S^2$ this parameter can be rewritten as

$$R_p = \frac{P/\varepsilon}{0.3\text{Re}_t^{1/2}} = \frac{P/\varepsilon}{0.3(\varepsilon/v)^{1/2}} = \frac{-\overline{u'v'}}{0.3k}R$$

$$\dots\dots\dots (18)$$

The alternative parameter R_p can b seen to be proportional to the parameter R multiplied by the structure parameter $\overline{u'v'}/k$ and the factor 0.3 has been introduced into the definition of R_p in order to make R_p and R the same when the structure parameter assumes a value of 0.3. The parameter R_p also represents a timescale ratio, namely the ratio of the timescale of the dissipating motion to the timescale P/k involving the production of turbulence. The variation of the parameter R_p in the channel flow

is also shown in figure 10. It can be seen to rise less steeply near the wall, which makes it more suited as modeling parameter as will be discussed in the next section.

6. Modeling the terms in the ε-equation

In order to turn the exact ε-equation into an equation that can be used in a turbulence model, the source and sink terms as well as the turbulent diffusion terms need to be modeled. As mentioned already, the sum of the source and sink terms is much smaller than the actual terms but it is still finite and in channel flow it is balanced by the equally small diffusion term. Models for the source and sink terms are considered first, and the starting point is the generally used basic model for high Reynolds-number (or low- R) situations where only P_ε^4-$Y$is left. This difference is modeled as (see e.g. Launder, Reece & Rodi 1975)

$$P_\varepsilon^4 - Y = \left(C_{\varepsilon 1}\frac{P}{\varepsilon} - C_{\varepsilon 2} \right)\frac{\varepsilon^2}{k} \quad \dots (19)$$

where P is the production of turbulent energy, that is the energy input into the low wavenumber part of the spectrum. The model relation (19) is compared in figure 11 with $P_\varepsilon^1+P_\varepsilon^2+ P_\varepsilon^3+P_\varepsilon^4$-$Y$ and in figure 14 with the sum of all source and sink terms ($C_{\varepsilon 2}$ is multiplied by the damping function f_2 of SM according to table 2, but f_2 is effective only for $y^+<$12). Depending somewhat on the constants $C_{\varepsilon 1}$ and $C_{\varepsilon 2}$ used, the basic model can be seen to simulate fairly well the sum of source and sink terms away from the wall, where P_ε^1, P_ε^2 and P_ε^3 are unimportant. The question now is how to bring in the influence of the production terms P_ε^1, P_ε^2 and P_ε^3 and the consequential increase in the destruction term Y. The terms P_ε^1 and P_ε^2 involving

the mean strain rate (first derivatives of velocities) are treated separately from the term P_ε^3 involving second derivatives.

6.1. Modeling the effect of P_ε^1 and P_ε

One possibility would be to add modeled terms of P_ε^1 and P_ε^2. P_ε^3 can be expressed as $-\varepsilon_{ij} U_{i,j}$, where ε_{ij} is the dissipation rate of the Reynolds-stress component $\overline{u_i'v_j'}$; this term is therefore closely related to $(\varepsilon^2/k)(P/\varepsilon)$ and hence effectively increases the value of the coefficient $C_{\varepsilon l}$ in (19), depending on P/ε. With such modeling of P_ε^1, and similarly of P_ε^2, the sink term would have to be increased drastically in order to account for the adjustment of Y due to the extra production by P_ε^1 and P_ε^2. As an alternative, the suggestion is therefore made here that the influence of the combined effect of P_ε^1 and P_ε^2 and Y be modeled, which increases somewhat the sink term in the ε-equation. Both timescale ratios R and R_p were tested as parameters to account for this effect, and the parameter R was found not to correlate too well. The close relation of P_ε^1 to the ratio of production to dissipation, P/ε, suggests that this ratio is an important parameter, and, in fact, the parameter R_p involving P/ε was found to be suitable.

　The combined effect of P_ε^1, P_ε^2 and the increase in Y is accounted for in the new model by multiplying the coefficient $C_{\varepsilon 2}$ in the sink term of (19) by the following function:

$$f_3 = \exp\left(2R_p^3\right) \qquad \textbf{(20)}$$

This was obtained by fitting the exponential function to the DNS data of figure 11.

The effect of this function can be seen in figure 11; it is restricted to the near-wall region of $y^+ < 30$.
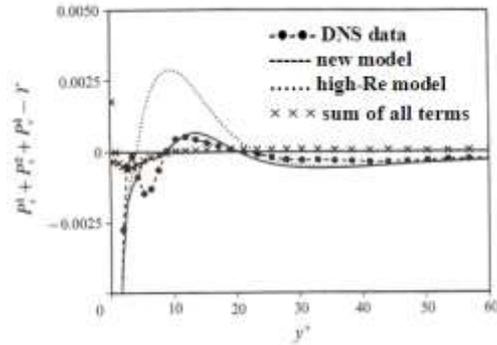

FIGURE 11. New model for source/sink terms $P_\varepsilon^1 + P_\varepsilon^2 + P_\varepsilon^3 + P_\varepsilon^4 - Y$ compared with DNS data $(Re, = 395)$.

The new model simulates quite well the distribution of the source and sink terms $P_\varepsilon^1 + P_\varepsilon^2 + P_\varepsilon^3 + P_\varepsilon^4 - Y$ down to $y^+ \approx 8$, below which the DNS results are not very reliable anyway. It is also in this region where the sink term in (19) has to be multiplied by another function f_2 which approaches the wall as y^2. Note that LB's f_2 function (see table 2) is of this type, and that Hanjalic & Launder (1976) and SM achieved this effect by replacing ε^2 in (19) by $\varepsilon\tilde{\varepsilon}$. Since the DNS-based-ε-budget terms are not accurate very near the wall, the f_2-function could not be determined directly from the DNS data and no proposal can be made here (we used the proposal of SM in figures 11 and *14a)*. Michelassi, Rodi & Zhu (1992) proposed an f_2-function that works in calculations with the present model for the high-*Re* channel flow. They also found that the proposal where the same f_2 is used as in SM (see table 2) was not entirely satisfactory in conjunction with the present model.

6.2. Bardina's model

Bardina (1988) suggested that the influence of high shear characterized by

58

high values of the parameter *R* could be accounted for by adding an extra term to the *ε*-equation which involves the mean rotation Ω. This model suggestion is based on his previous work on turbulence under the influence of rotation (Bardina, Ferziger & Reynolds 1983). The extra term is

$$-\left(C_{\Omega 1}\frac{P}{\varepsilon}+C_{\Omega 2}\right)\frac{\Omega k}{\varepsilon}\frac{\varepsilon^2}{k} \qquad (21)$$

In his study on homogeneous shear layers, Bardina (1988) found that with this extra term (with constants $C_{\Omega 1}$ = 0.015 and $C_{\Omega 2}$ = 0.15) the sum of the source and sink terms (P_ε^1+P_ε^2+ P_ε^3+P_ε^4-Y) are modeled quite well for the high shear case also; without the extra term, only the low-shear situation was simulated well. It should be added here that the high-shear case was at a rather low Reynolds number. Bardina's model, with his constants, was applied to the channel flow, and the results are shown in figure 12. The model can be seen to have the correct trend, namely to reduce the sum of source and sink terms in the *ε*-equation near the wall, but the reduction is somewhat excessive. Hence there appears to be too much sensitivity to the mean rotation, which in the present case is the velocity gradient $U_{,y}$ Perhaps this oversensitivity could be remedied by multiplying the extra term (21), which does not include any Reynolds-number dependence, by a suitable function of the turbulent Reynolds number Re_t.
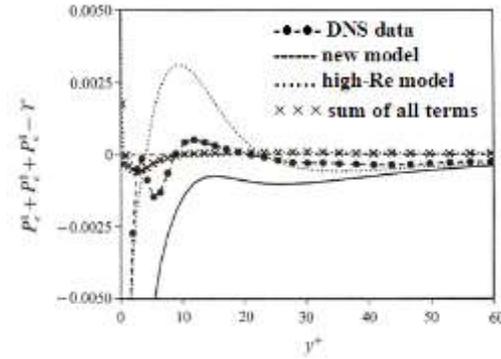

FIGURE 12. Bardina's model for source/sink terms P_ε^1+P_ε^2+ P_ε^3+P_ε^4-Y compared with DNS data (Re, = 395) .

6.3. Modeling of P_ε^3

The production term P_ε^3 involving second derivatives of the mean velocity is small compared with the other source and sink terms, but it is comparable with their sum and also with the turbulent diffusion term (see figure 8). Hence it is important to represent realistically this term in a model also. Hanjalic & Launder (1976) used a generalized gradient approximation for the fluctuating velocity gradients $u'_{i,j}$ appearing in the turbulence correlation in the P_ε^3 term and expressed these gradients in terms of second derivatives of the mean velocity. They arrived at a model expression which, for the special case of channel flow, reads

$$P_\varepsilon^3 = C_{\varepsilon v}\, 2v\frac{\overline{v'^2}k}{\varepsilon}\left(U,_{yy}\right)^2 \qquad (22)$$

With $\overline{v'^2}$ replaced by k and $v_t \propto k^2/\varepsilon$, the model used by LS results:

$$P_\varepsilon^3 = 2v v_t\left(U,_{yy}\right)^2 \qquad (23)$$

The P_ε^3 distribution resulting from this model is compared in figure 13 with the DNS data. The model can be seen to have two problems. One is that the size of P_ε^3 is significantly over predicted; this could be fixed by using a different

constant. The other more fundamental problem is that the LS model predicts P_ε^3 to be always positive while the DNS data show that P_ε^3 becomes negative near the wall. It can be shown from a series expansion of the fluctuating velocities u' and v' as given in Mansour *et al. (1988)* that the correlation $\overline{v'u'}_{,y}$, which is the only contribution to P_ε^3 in channel flow, should behave as $\left(\overline{u'v'}\right)_{,y}$ near the wall, i.e. as y^2, and should be negative. This confirms the behavior resulting from the DNS data. In fact, the Chebychev transform of $p\sim$ reveals that the term is well resolved and that the only source of error will be from the number of samples used. Considering that this term is important close to the wall where the turbulent eddies are small, that each flow field yields two planes with 256 x 192 samples, and that we averaged over 19 fields, we consider that the distribution given in figure 13 is converged.
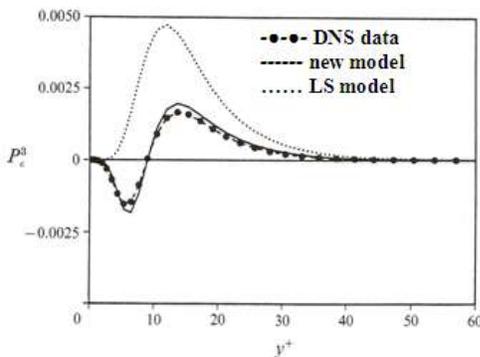

FIGURE 13. Model for P:-production compared with DNS data *(Re, = 395)*.

Because of the fundamental problems with the LS model for P_ε^3, an improved model was developed. To this end, an exact equation for the correlation $\overline{v'_k u'_{i,j}}$ appearing in the P_ε^3 definition was derived by manipulating the Navier-Stokes equations. For modeling purposes, it was then assumed that the

correlation is related to the source terms in the exact equation involving mean velocity derivatives. For channel flow only the correlation $\overline{v'u'}_{,y}$ is of interest, and the main source terms in the equation for this correlation are

$$-\overline{v'^2}U_{,yy} - \frac{1}{2}\overline{v'^2}_{,y}U_{,y} \qquad (24)$$

Multiplying these terms by a timescale $k/\tilde{\varepsilon}$ for dimensional reasons and assuming $\overline{v'^2} \propto k$ and $k^2/\tilde{\varepsilon} \propto v_t$ in the context of a *k-ε* eddy-viscosity model, and allowing for different multiplying constants for each of the terms in (24), the following model is obtained for shear-layer flows:

$$P_\varepsilon^3 = -2\overline{v'u'}_{,y}U_{,yy} = C_1^3 2v v_t \left(U_{,yy}\right)^2 + C_2^3 v_t \frac{k}{\varepsilon} k_{,y} U_{,y} U_{,yy}. \qquad (25)$$

The first term can be seen to be the model of LS which is always positive. The second term is negative near the wall as desired and turns positive further away from the wall. This term also has the correct near-wall behavior, namely it approaches the wall as y^2. Adjusting the constants C_1^3 and C_2^3 to best fit the DNS data (C_1^3=0.5, C_2^3=0.006) the curve given in figure 13 follows. The fit can be seen to be very good.

6.4. Model performance for sum of all source/sink terms

The model for P_ε^3 is now combined with the previously discussed model for the other source and sink terms, including the R_p function (20). The performance of the resulting model for the sum of all source and sink terms is shown in figure 14(a). The agreement between the model prediction and the DNS data is good down to $y^+\approx 8$, below which the DNS data are not so reliable anyway. It should be

mentioned here once more that in this region the sink term in (19) needs to be multiplied by a damping function f_2 which could not be determined from the DNS data. It is of interest to see how this performance compares with that of the five selected existing models: CH, LS, LB, SM and NT. Hence, in figure l4(*b-f*) the models for the sum of all source and sink terms in the ε-equations due to CH, LS, LB, SM and NT are compared with the DNS data.
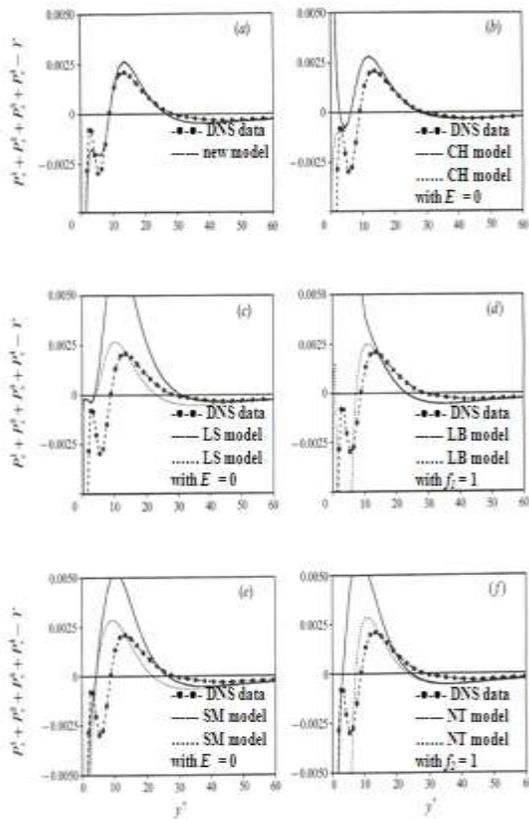

FIGURE 14. Models for all source/sink terms in the ε-equation compared with DNS data for channel flow ($Re_\tau = 395$).

For $y^+\leq40$, all models behave basically the same, because here the extra terms ε and functions f_1 and f_2 are not effective. In the range $20\leq y^+\leq40$, the CH model is superior because it uses different constants $C_{\varepsilon 1}$ and $C_{\varepsilon 2}$ than the other

models (see table 2), which seem to be more suitable in channel flow. However, these constants may not be so suitable for other flows, e.g. free shear layers, for which the constants $C_{\varepsilon 1}$ and $C_{\varepsilon 2}$ used in the other models were optimized. Even below $y^+=20$, the CH model is quite reasonable, but it is not as accurate as the new model, the results for which are shown in figure l4(a). The *E-term* in the CH model is effective only below $y^+\approx5$ which shows that the basic model of (19) without an extra *E-term* or f_1 and f_2 functions is quite reasonable, especially when suitable $C_{\varepsilon 1}$ and $C_{\varepsilon 2}$ constants are chosen. Figure l4(c) shows that the LS model predicts far too high values of the source/sink terms near the wall, which is due to the *E-term* in their model t equation representing the P_ε^3- production (see also figure 13).
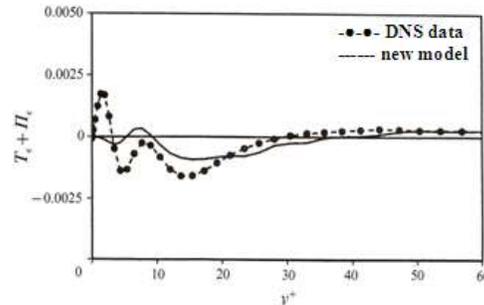

FIGURE 15. Model for diffusion term $T_\varepsilon+\Pi_\varepsilon$ in ε-equation compared with DNS data ($Re_\tau = 395$) .

The SM model which used the same *E-term* formulation but a factor of 2 smaller than LS, still over predicts the source/sink terms. Overall, the model behavior is better without this term in both cases. Similarly, the f_1-function in the LB model which increases the production of ε has the wrong effect because f_1 assumes very large values near the wall. Again, the model behavior is better without this function. Finally, the f_2-function in the NT model can also

61

be seen to lead to excessive values of the source/sink term near the wall.

6.5. Diffusion model

Finally, the diffusion model generally used in the T_ε-equation is tested against the DNS data in figure 15. In the channel flow considered, the diffusion model reads

$$T_\varepsilon = \left(\frac{v_t}{\sigma_\varepsilon} \varepsilon_{,y} \right)_{,y} \qquad (26)$$

and the adjustable constant σ_ε is normally taken as 1.3. Figure 15 shows that this

model simulates the distribution of the diffusion term fairly well, even though the accuracy is not so good near the wall.

7. Conclusions

From the evaluation of DNS data for channel and boundary-layer flow it was found that away from the wall the coefficient C_μ depends on the type of flow and on the Reynolds number and varies in the bulk of the flows in the range 0.07 to 0.12. Considering only regions where the structure parameter $\overline{u'v'}/k$ is approximately constant, there is a clear dependence of C_μ on P/ε as given by relation (5). A fixed value of C_μ = 0.09 is therefore not very accurate for all situations and a damping function f_μ designed to recover this value away from the wall cannot be in good agreement with all DNS data examined. Nevertheless, some general conclusions can be drawn on existing model functions: the f_μ function of Chien (CH) rises much too slowly, the function due to Launder & Sharma (LS) increases far too fast with distance from the wall, the functions due to Lam & Bremhorst (LB) and Shih & Mansour (SM) perform well, but approach unity too slowly,

while the function of Nagano & Tagawa (NT) fits the high-*Re* channel data fairly well. An even better fit is achieved in this paper with a new function of the dimensionless wall distance y^+. A damping function was found unnecessary except very close to the wall ($y^+ < 10$) when $(\overline{v'^2})^{1/2}$ is used as velOCity scale instead of $k^{1/2}$ in the eddy-viscosity relation, as suggested by Durbin (1990).

The ε-budget was determined from Kim (1990, unpublished data) for channel flow at Re_τ = 395. This was found reliable down to a wall distance of $y^+ \approx 8$, as the calculated imbalance term is very small for $y^+ > 8$. As expected, the main terms in the ε-budget are the vortex-stretching-production term P_ε^4 and the viscous destruction term *Y,* but near the wall the production terms P_ε^1 and P_ε^2 involving the mean strain rate are of similar magnitude. These production terms were found to cause the viscous destruction term to increase near the wall so that the sum of all source and sink terms is small compared with the main individual source and sink terms over the whole channel depth. The turbulent diffusion and the P_ε^3 term involving second derivatives of the mean velocity are of the same small magnitude. Through scaling considerations it was shown that the difference of the main source/sink terms, P_ε^4-*Y,* and the transport terms (here only turbulent diffusion) are independent of Reynolds number and also that the ratio of P_ε^1 and P_ε^2 to these terms is given by a parameter *R* involving the strain rate and the Reynolds number Re_t. This parameter represents the ratio of the timescale of the dissipating motion to the timescale of the mean strain field.

A new model was proposed and tested against the DNS channel data which

simulates the net effect of the production terms P_ε^1 and P_ε^2 and the consequential increase in the destruction term Y. In this new model, the sink term in the ε-equation is increased slightly near the wall through a parameter Rp involving the ratio of production to dissipation, P/ε, and the turbulent Reynolds number Re_t. A new model for the source term P_ε^3 was also derived, based on the production terms in the exact equation for the turbulence correlation appearing in P_ε^3. Altogether, the new models simulate the sum of all source and sink terms in the channel flow very well down to $y^+ \approx 8$. Judging from the comparison with the DNS data, the new model is better than the existing models investigated. The CH model is not as accurate near the wall, but it is still quite reasonable, while the LS, LB, SM and NT models produce too large source terms near the wall. The new model proposals comprising a new f_μ function and new suggestions for the source/sink terms in the ε-equation need to be complemented by a damping function f_2 multiplying the sink term in the model ε-equation very near the wall ($y^+ < 5$) before they can be used in actual flow calculations. This was done by Michelassi *et al.* (1992) who used the model to calculate the channel and boundary layer flows at the same Reynolds numbers as the DNS data used in the present paper. With a slightly re-optimized form they obtained good agreement with the DNS data, for the first time for the e-distribution also. The new model should now be tested for other flows.

REFERENCES

BARDINA, J. 1988 Turbulence modelling based on direct simulation of the Navier-Stokes equations. First National Fluid Dynamics Congress, Cincinnati, Ohio, A/AA *88-3747-CP*.

BARDINA, J., FERZIGER, J. H. & REYNOLDS, W. C. 1983 Improved turbulence models based on large eddy simulation of homogeneous incompressible, turbulent flows. *Rep. TF-19*. Thermosciences Division, Department of Mechanical Engineering, Stanford University.

CHIEN, K.-Y. 1982 Predictions of channel and boundary-layer flows with a low-Reynolds-number turbulence model. *A/AA* J. 20, 33-38 (referred to herein as CH)

DURBIN, P. A. 2003 Near-wall turbulence closure modeling without 'damping functions'. *CTR* manuscript 112. Center for Turbulence Research, Stanford University.

HANJALI, K. & LAUNDER, B. E. 1976 Contribution towards a Reynolds-stress closure for low Reynolds-number turbulence. *J.* Fluid Mech. 74, 593-610.

KIM, J., MOIN, P. & MaSER, R. 1987 Turbulence statistics in fully developed channel flow at low Reynolds number. *J. Fluid Mech.* 177, 133-166.

LAM, C. K. G. & BREMHORST, K. A. 1981 Modified form of the *k-ε* model for predicting wall turbulence. *Trans. ASME* I: *J. Fluids Engng* 103, 456-460 (referred to herein as LB).

LAUFER, J. 1954 The structure of turbulence in fully developed pipe flow. *NACA Rep. 1174.* LAUNDER, B. E. 1986 Low-Reynolds-number turbulence near walls. *Rep.* TFD/86/4. UMIST, Manchester.

LAUNDER, B. E., REECE, G. J. & RODI, W. 1975 Progress in the development of a

Reynolds-stress turbulence closure. *J. Fluid Mech.* 68, 537-566.

LAUNDER, B. E. & SHARMA, B. 1. 1974 Application of the energy-dissipation model of turbulence to the calculation of flow near a spinning disk. *Lett. Heat Mass Transfer* 1, 131-138 (referred to herein as LS).

MANSOUR, N. N. 2001 The use of direct numerical simulation data in turbulence modelling. *29th* Aerospace Sciences Meeting, Reno, Nevada, AIAA 91-0221.

MANSOUR, N. N., KIM, J. & MOIN, P. 1988. Reynolds-stress and dissipation rate budgets in a turbulent channel flow. *J.* Fluid Mech. 194, 15-44.

MICHELASSI, V., RODI, W. & ZHU, J. 2002 Testing a low Reynolds number *k-ε* turbulence model based on direct simulation data. *Rep.* SFB 2l0/T /83, University of Karlsruhe, Germany (also, to appear in abbreviated form as a Technical Note in *AIAA J.).*

NAGANa, Y. & TAGAWA, M. 1990 An improved *k-ε* model for boundary layer flows. *Trans. ASME* I: *J. Fluids Engng* 112, 33-39 (referred to herein as NT).

PATEL, V. C., RODI, W. & SCHEUERER, G. 1985 Turbulence models for near-wall and low-Reynolds number flows: A review. *AIAA J.* 23, 1308-1319.

RODI, W. 1971 On the equation governing the rate of turbulent energy dissipation. *Rep.* TM/TN/ A/14, Imperial College of Science and Technology, Department of Mechanical Engineering, London.

RODI, W. 2000 A note on the empirical constant in the Kolmogorov-Prandtl eddy-viscosity expression. *Trans. ASME* I: *J. Fluids Engng* 97, 386-389.

SHIH, T.-H. & MANSOUR, N. N. 1990 Modelling of near-wall turbulence. In *Engineering Turbulence Modelling and Experiments* (ed. W. Rodi & E. N. Ganic). Elsevier (referred to herein as SM).

SPALART, P. R. 1988 Direct simulation of a turbulent boundary layer up to *Re =* 1410. *J. Fluid Mech.* 187, 61-98.

TENNEKES, H. & LUMLEY, J. L. 1972 A First Course in Turbulence. The MIT Press.

نموذج ε–k لأعداد رينولد منخفضة باستخدام بيانات المحاكاة المباشرة

أحمد عبد الحسين عودة

جامعة ذي قار– كلية العلوم– قسم علوم الحاسبات

المستخلص:

في هذه الدراسة يتم حساب الثابت C_μ ودالة الإخماد قرب الجدار f_μ في الدوامات اللزجة نسبة إلى نموذج $k\text{-}\varepsilon$ من بيانات المحاكاة العددية المباشرة (DNS) لتطوير جريان القنوات والطبقات المتاخمة عند اثنين من أعداد رينولد. يوجد العديد من نماذج دالة الإخماد f_μ ويتم مقارنتها مع بيانات المحاكاة العددية المباشرة وتم ملائمة الدالة الجديدة عند بيانات جريان القنوات بأعداد عالية من أعداد رينولد. موازنة ε تم احتسابها لجريان قناة متكامل. القيمة النسبية لحدود معادلة ε تم تحليلها بمساعدة طرق المقايسة والعوامل التي تتحكم في القيمة تم تثبيتها. وبالمقارنة مع نماذج مجموع حدود المصادر والمخارج في معادلة ε مع بيانات المحاكاة العددية المباشرة اثبت النموذج الجديد كفاءته.